

Electronic Supporting Information

Magnetostructural relationship for μ_2 -phenoxido bridged ferric dimers

Fei Yu,^a Zi-Heng Cao,^a Jing-Yuan Ge,^a Yi-Chen Sun,^b Zhong-Wen Ouyang,^b Jing-Lin Zuo,^{*a} Zhenxing Wang,^{*b} and Mohamedally Kurmoo^c

^a State Key Laboratory of Coordination Chemistry, School of Chemistry and Chemical Engineering, Collaborative Innovation Center of Advanced Microstructures, Nanjing University, Nanjing, 210093, P. R. China.

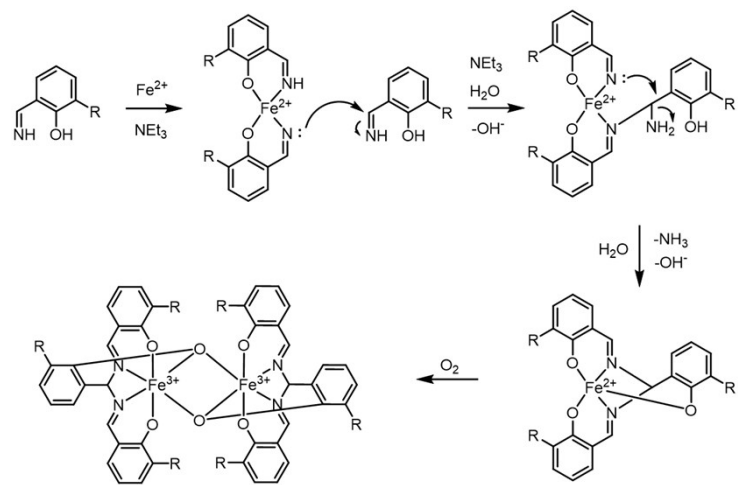
^b Wuhan National High Magnetic Field Center, Huazhong University of Science and Technology, Wuhan, 430074, P. R. China.

^c Institut de Chimie de Strasbourg, Université de Strasbourg, CNRS-UMR 7177, 4 rue Blaise Pascal, 67008 Cedex Strasbourg, France.

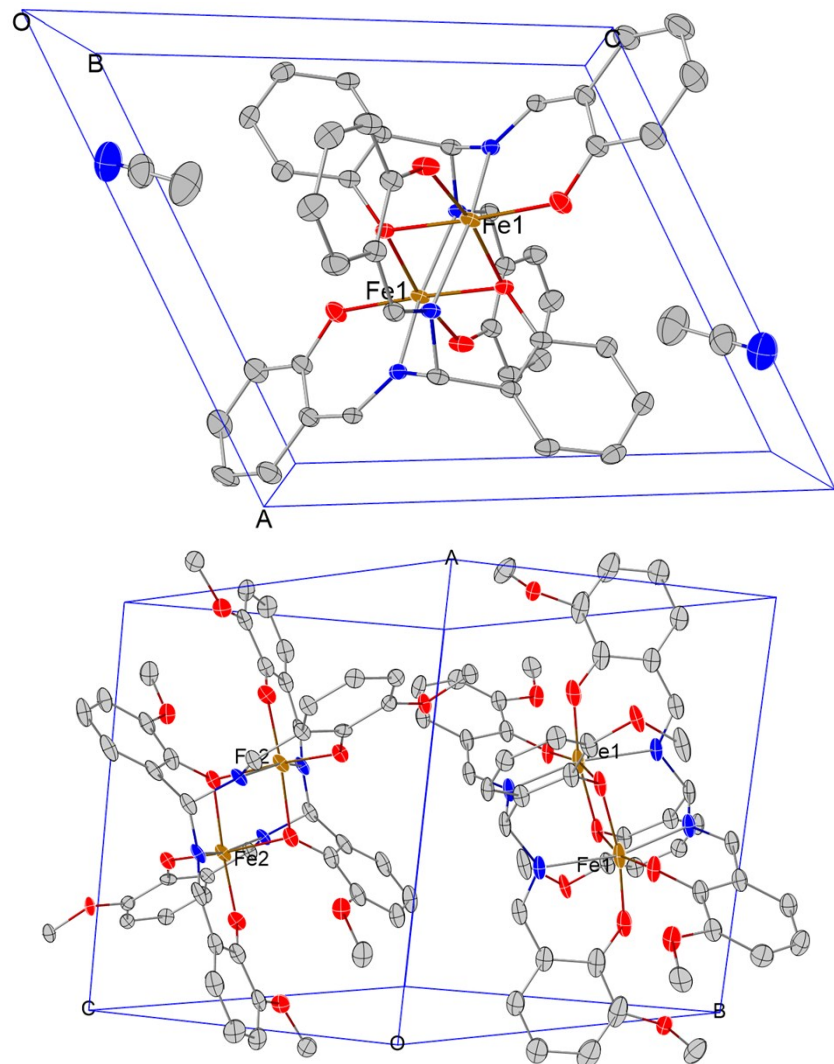
* To whom correspondence should be addressed. Email: zuojl@nju.edu.cn (JLZ), zxwang@hust.edu.cn (ZW).

Caption of Content

- 1. Scheme S1.** Proposed Reaction Leading to ligands.
- 2. Fig. S1** Structures of the molecular units in **1**, **2** and **3**.
- 3. Table S1** Selected bond lengths (\AA) and angles ($^{\circ}$) for **1**, **2** and **3**.
- 4. Table S2** Hydrogen-bond geometry (\AA , $^{\circ}$) for **(2)**.
- 5. Table S3** Hydrogen-bond geometry (\AA , $^{\circ}$) for **(3)**.
- 6. Table S4** Structural and magnetic data for *bis*(μ_2 -phenoxido)diiron(III) complexes
- 7. Fig. S2** TGA plots for **1**, **2** and **3**.
- 8. Fig. S3** PXRD patterns for **1**, **2** and **3**.
- 9. Fig. S4** Raman spectra of **1**, **2** and **3**.
- 10. Fig. S5** Isothermal magnetizations for **1**, **2** and **3** at 1.8 K.
- 11. Fig. S6** Zeeman splitting of the Energy levels for **1**, **2** and **3**.



Scheme S1. Proposed Reaction Leading to ligands $\text{H}_2\text{L}-\text{R}$ ($\text{H}_2\text{L}-\text{H}$, $\text{H}_2\text{L}-\text{OCH}_3$ and $\text{H}_2\text{L}-\text{OC}_2\text{H}_5$) for complexes **1**, **2** and **3**.



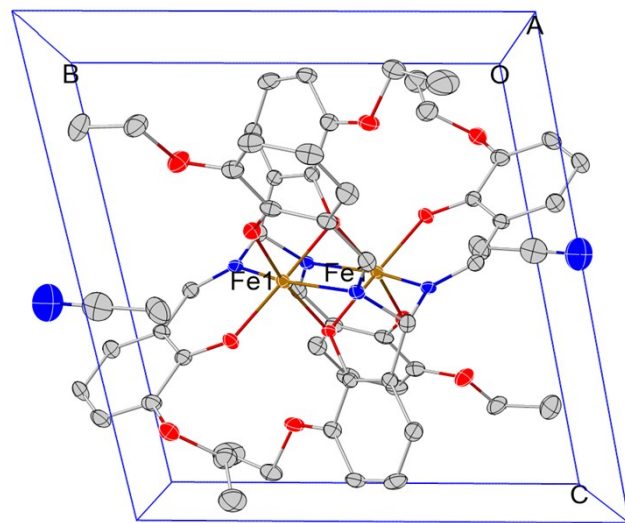


Fig. S1 Structures of the molecular units in **1**, **2** and **3**.

Table S1 Selected bond lengths (\AA) and angles ($^\circ$) for **1**, **2** and **3**.

1			
Fe1-O1	2.026 (1)	Fe1-O1 ⁱ	2.061 (2)
Fe1-O2	1.903 (1)	Fe1-O3 ⁱ	1.915 (2)
Fe1-N1	2.161(2)	Fe1-N2 ⁱ	2.147(2)
Fe1 ⁱ -O1-Fe1	98.01(6)	O1-Fe1-O2	169.81(6)
O1-Fe1-O3 ⁱ	91.86(6)	O1-Fe1-O1 ⁱ	81.99(6)
O1-Fe1-N1	82.34(6)	O1-Fe1-N2 ⁱ	86.34(6)
O1 ⁱ -Fe1-N1	81.80 (6)	O1 ⁱ -Fe1-O2	93.66(6)
O1 ⁱ -Fe1-O3 ⁱ	167.39(6)	O2-Fe1-O3 ⁱ	94.10(7)
O2-Fe1-N2 ⁱ	102.23(6)	O2-Fe1-N1	87.94(6)
O3 ⁱ -Fe1-N1	108.39(6)	O3 ⁱ -Fe1-N2 ⁱ	86.75(6)
N1-Fe1- N2 ⁱ	161.28(6)	O1 ⁱ -Fe1-N2 ⁱ	81.90 (6)
2			
Fe1-O1	2.040(3)	Fe1-O1 ⁱ	2.066(2)
Fe1-O3	1.905(3)	Fe1-O5 ⁱ	1.930(3)
Fe1-N1	2.164(3)	Fe1-N2 ⁱ	2.129(3)
Fe1 ⁱ -O1	2.066(2)	Fe1 ⁱ -O5	1.930(3)
Fe1 ⁱ -N2	2.129(3)	Fe2-O11 ⁱⁱ	1.911(3)
Fe2-O9	1.904(3)	Fe2-O7	2.020(3)
Fe2-O7 ⁱⁱ	2.091(3)	Fe2-N4 ⁱⁱ	2.124(3)
Fe2-N3	2.137(3)	Fe2 ⁱⁱ -O7	2.091(3)
Fe2 ⁱⁱ -O11	1.912(3)	Fe2 ⁱⁱ -N4	2.124(3)
Fe1-O1-Fe1 ⁱ	97.03(12)	Fe2-O7-Fe2 ⁱⁱ	97.17(11)
O1-Fe1-O3	168.83(7)	O1-Fe1-O5 ⁱ	91.90(12)
O1-Fe1-N1	81.97(12)	O1-Fe1-O1 ⁱ	82.97(12)
O1 ⁱ -Fe1-N1	82.67(11)	O1-Fe1-N2 ⁱ	87.59(12)
O1 ⁱ -Fe1-O5 ⁱ	167.10(12)	O1 ⁱ -Fe1-O3	94.89(12)
O3-Fe1-O1	169.33(11)	O3-Fe1-O5 ⁱ	92.26(12)
O3-Fe1-N2 ⁱ	102.47(13)	O1 ⁱ -Fe1-N2 ⁱ	81.51(11)
O5 ⁱ -Fe1-N1	108.41(11)	O3-Fe1-N1	87.39(13)
N1-Fe1- N2 ⁱ	161.99(12)	O5 ⁱ -Fe1-N2 ⁱ	86.48(11)

O9-Fe2-O11 ⁱⁱ	95.24(12)	O9-Fe2-O7	169.89(11)
O11 ⁱⁱ -Fe2-O7	93.25(11)	O9-Fe2-O7 ⁱⁱ	89.64(11)
O11 ⁱⁱ -Fe2-O7 ⁱⁱ	169.92(10)	O7-Fe2-O7 ⁱⁱ	82.83(11)
O9-Fe2-N4 ⁱⁱ	99.16(12)	O11 ⁱⁱ -Fe2-N4 ⁱⁱ	88.79(11)
O7-Fe2-N4 ⁱⁱ	86.46(11)	O7 ⁱⁱ -Fe2-N4 ⁱⁱ	81.72(11)
O9-Fe2-N3	89.10(12)	O11 ⁱⁱ -Fe2-N3	107.96(12)
O7-Fe2-N3	83.08(11)	O7 ⁱⁱ -Fe2-N3	80.88(11)
N4 ⁱⁱ -Fe2-N3	160.67(12)		
		3	
Fe1-O1	2.049(2)	Fe1-O1 ⁱ	2.048(2)
Fe1-O3	1.913(2)	Fe1-O5 ⁱ	1.919(2)
Fe1-N1	2.166(2)	Fe1-N2 ⁱ	2.146(2)
Fe1 ⁱ -O1-Fe1	98.53(7)	O1-Fe1-O3	168.83(7)
O1-Fe1-O5 ⁱ	92.41(7)	O1-Fe1-O1 ⁱ	81.47(7)
O1-Fe1-N1	81.78(7)	O1-Fe1-N2 ⁱ	84.83(7)
O1 ⁱ -Fe1-N1	81.74(7)	O1 ⁱ -Fe1-O3	94.49(7)
O1 ⁱ -Fe1-O5 ⁱ	168.27(7)	O3-Fe1-O5 ⁱ	93.29(8)
O3-Fe1-N2 ⁱ	105.03(8)	O3-Fe1-N1	87.34(8)
O5 ⁱ -Fe1-N1	107.41(7)	O5 ⁱ -Fe1-N2 ⁱ	87.22(7)
N1-Fe1- N2 ⁱ	160.49(8)	O1 ⁱ -Fe1-N2 ⁱ	82.28 (7)

Symmetry codes for **1**: Symmetry code: (i) - $x+1$, - $y+1$, - $z+1$; **2**: Symmetry code: (i) - $x+1$, - $y+1$, - $z+2$; (ii) - $x+1$, - y , - $z+1$; **3**: Symmetry code: (i) - $x+1$, - $y+1$, - $z+1$.

Table S2 Hydrogen-bond geometry (\AA , $^\circ$) for **(2)**. (D, donor atom; A, acceptor atom).

D—H···A	D—H	H···A	D···A	D—H···A
C7—H7B···O5 ⁱ	0.98	2.40	3.304(6)	154
C23—H23C···O10 ⁱⁱ	0.98	2.64	3.187(4)	115
C39—H39C···O9 ⁱⁱⁱ	0.98	2.52	3.409(5)	151
C40—H40···O2 ⁱ	0.95	2.48	3.338(5)	150
C47—H47C···O3 ^{iv}	0.98	2.51	3.395(5)	150

C47—H47···CO4 ^{iv}	0.98	2.45	3.191(8)	132
-----------------------------	------	------	----------	-----

Symmetry codes: (i) - $x+1$, - $y+1$, - $z+2$; (ii) - $x+1$, - y , - $z+1$; (iii) - $x+2$, - y , - $z+1$; (iv) - $x+1$, - y , - $z+2$.

Table S3 Hydrogen-bond geometry (\AA , $^\circ$) for (3). (D, donor atom; A, acceptor atom).

D—H···A	D—H	H···A	D···A	D—H···A
C25—H25B···O5	0.99	2.36	2.922(3)	115
C27—H27···N3 ⁱⁱ	0.95	2.45	3.399(4)	172
C29—H29A···O6	0.98	2.46	3.201(4)	133
C29—H29B···O3 ⁱ	0.98	2.39	3.330(4)	162
C29—H29B···O5	0.98	2.60	3.275(4)	126
C29—H29C···N3 ⁱⁱⁱ	0.98	2.50	3.335(5)	143

Symmetry codes: (i) - $x+1$, - $y+1$, - $z+1$; (ii) - $x+1$, - y , - $z+1$; (iii) - x , - y , - $z+1$.

Table S4 Structural and magnetic data for *bis*(μ_2 -oxido)diiron(III) complexes with separation ferromagnetic and antiferromagnetic ($H = -2JS_1 \cdot S_2$).

Complex	Fe···Fe/ \AA	Fe—O—Fe/ $^\circ$	$P/\text{\AA}^a$	$J_{\text{exp}}/\text{cm}^{-1}$	$J_{\text{eq}}/\text{cm}^{-1}\text{ }^b$	Ref.
<i>bis</i> (μ_2 -phenoxido)diiron(III) complexes						
[Fe ₂ (L-H) ₂]·2CH ₃ CN	3.085	98.02	2.044	+0.47	-4.85	This work
Fe ₂ (L-OCH ₃) ₂	3.076	97.03	2.066	+0.86	-3.82	This work
[Fe ₂ (L-OC ₂ H ₅) ₂]·2CH ₃ CN	3.105	98.53	2.048	-0.72	-4.79	This work
Fe ₂ (salmp) ₂ ^c	3.062	97.02	2.064	+1.21	-3.91	1
[FeL ¹ Cl] ₂ ^d	3.248	105.0	2.044	-6.51	-5.02	2
[FeL ² (MeOH)Cl] ₂ ^e	3.216	105.1	2.025	-7.71	-6.43	2
[FeL ³ Cl] ₂ ^f	3.186	105.6	1.999	-10.92	-8.91	2
[FeL ⁴ (MeOH)Cl] ₂ ^g	3.163	104.7	1.997	-8.02	-9.23	3
[Fe ₂ L ₂] ^h	3.321	108.9	2.043	-12.71	-5.11	4
[Fe ₂ L ₂] ⁱ	3.341	103.8	2.12	-6.44	-1.92	5
<i>bis</i> (μ_2 -alkoxido)diiron(III) complexes						

[Fe ₂ (L ₂)] ^j	3.125	101.05	2.024	-2.2	-6.5	6
[Fe(heidi)(H ₂ O)] ₂ ^k	3.119	104.3	1.9755	-13.4	-12.0	7
[Fe{N(PL) ₂) ₂ ala}] ₂ ²⁺ ^l	3.180	103.8	2.0205	-5.2	-6.8	8
[Fe ₂ (acac) ₄ (OEt) ₂] ^m	3.116	103.6	1.982	-11.0	-11.0	9
[Fe ₂ L(OEt)Cl ₂] ⁿ	3.114	104.3	1.991	-15.4	-9.9	9
[Fe ₂ L(OMe)Cl ₂] ^o	3.106	103.0	1.995	-16.3	-9.4	10
[Fe(cupf) ₂ (OMe)] ₂ ^p	3.075	102.4	1.9725	-14.0	-12.5	11
<i>bis(μ₂-hydroxido)diiron(III) complexes</i>						
[Fe(L)(OH)] ₂ ^q	3.085	100.7	2.002	-5.5	-7.7	12
[Fe(chel)(H ₂ O)(OH)] ₂ ^r	3.078	103.2	1.964	-7.3	-14.6	13
[Fe(L)(OH)] ₂ ^s	3.155	102.8	2.021	-10.4	-6.9	14
[Fe(dipic)(H ₂ O)(OH)] ₂ ^t	3.098	103.6	1.965	-11.4	-14.4	13
[Fe(Me ₂ Npic)(H ₂ O)(OH)] ₂ ^u	3.118	105.3	1.962	-11.7	-16.2	15

^a Half of the shortest super-exchange pathway between two Fe(III) ions.

^b Calculated using the exponential relationship $-J_{eq} = A \exp(BP)$ and the reported values $A = 8.763 \times 10^{11}$ and $B = -12.662$.¹¹

^c H₃salmp = 2-bis(salicylideneamino) methylphenol.

^d H₂L¹ = N-2-hydroxyphenyl-3-hydroxy-2-naphthaldimine.

^e H₂L² = N-2-hydroxy-4-chlorophenylsalicylaldimine.

^f H₂L³ = N-2-hydroxyphenylsalicylaldimine.

^g H₂L⁴ = N-2-hydroxy-4-chlorophenyl-3-hydroxy-2-naphthaldimine.

^h H₃L = C₆H₂(CH₃)(OH){[C(CH₃)₃]₂(OH)NCH}₂.

ⁱ N,N'-bis-(5-chlorosalicylidene)-2-methylpropane-1,2-diamine.

^j H₃L = 1-Salicylideneamino-3-salicylaminopropan-2-ol.

^k H₃heidi = [N,N'-Di(2-acetate)-N-2-(hydroxyethyl)]amine.

^l H₂N(PL)₂ala = α,3-Dihydroxy-β-{[(3-hydroxy-5-hydroxymethyl-2-methyl-4-pyridyl)methylene]amino}-5-hydroxymethyl-α,2 dimethyl-4-pyridylpropanoic acid.

^m acac = Pentane-2,4-dionate.

ⁿ H₃L = 1,4-Piperazinediyl-bis(N-ethylenesalicylaldimine).

^o H₂L = pimelyl-bis(N-isopropylhydroxamic acid).

^p Hcupf = PhN(OH)NO (cupferron).

^q H₂L = macrocyclic tetraaminodiphenol ligand.

^r H₂chel = 4-hydroxo-2,6-pyridine-dicarboxylate.

^s H₂L = N,N'-ethylenebis(salicylamine).

^t H₂dipic = 2,6-pyridinedicarboxylate.

^u H₂Me₂Npic = 4-(dimethyl-amino)-2,6-pyridinedicarboxylate.

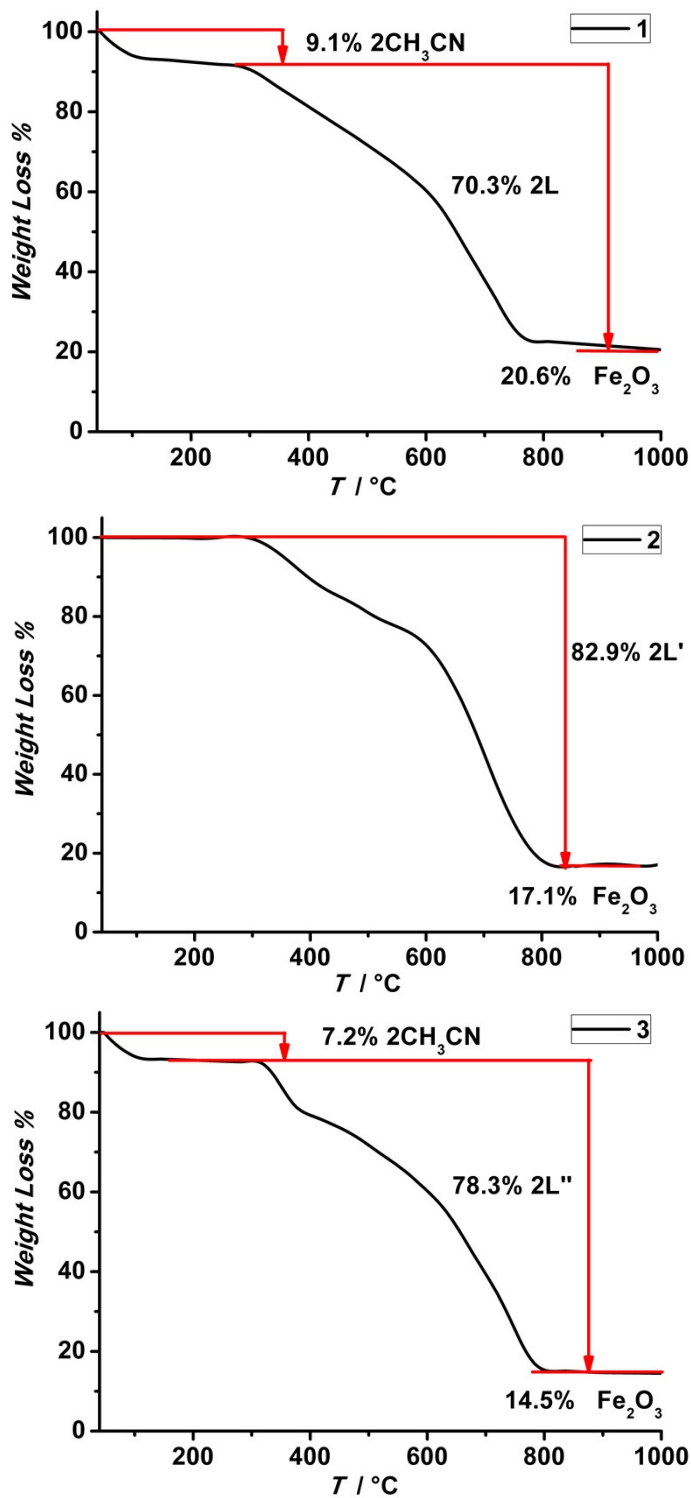
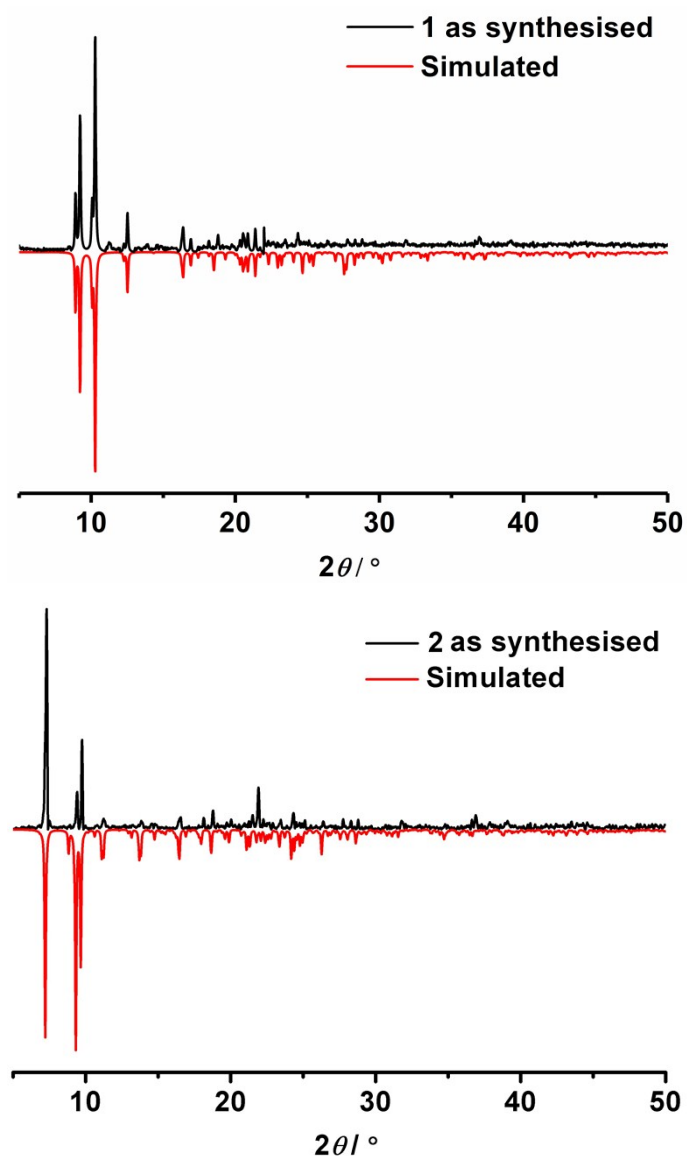


Fig. S2 TGA plots for **1**, **2** and **3**. For **1**, there are two steps of weight loss. The first one from 40 to 310 $^{\circ}\text{C}$ corresponds to the loss of the acetonitrile molecule (obs. 9.1 %, calc. 9.3 %), Then the desolvated network becomes unstable above 310 $^{\circ}\text{C}$. The second weight loss of 70.3 % (calc. for Fe₂O₃ 72.6 %) from 410 to 800 $^{\circ}\text{C}$ corresponds to the decomposition of the compound. For **2**, the complex is stable until 310 $^{\circ}\text{C}$. The weight loss of 82.9 % in the range of 310 to 820 $^{\circ}\text{C}$ corresponds to the

decomposition to Fe_2O_3 (calc. 83.7%). For **3**, there are two steps of weight loss. The first one from 40 to 315 °C corresponds to the loss of the acetonitrile molecule (obs. 7.2 %, calc. 7.1 %). Then the desolvated network becomes unstable above 315 °C. The second weight loss of 78.3 % (calc. for Fe_2O_3 78.9 %) from 410 to 800 °C corresponds to the decomposition of the compound.



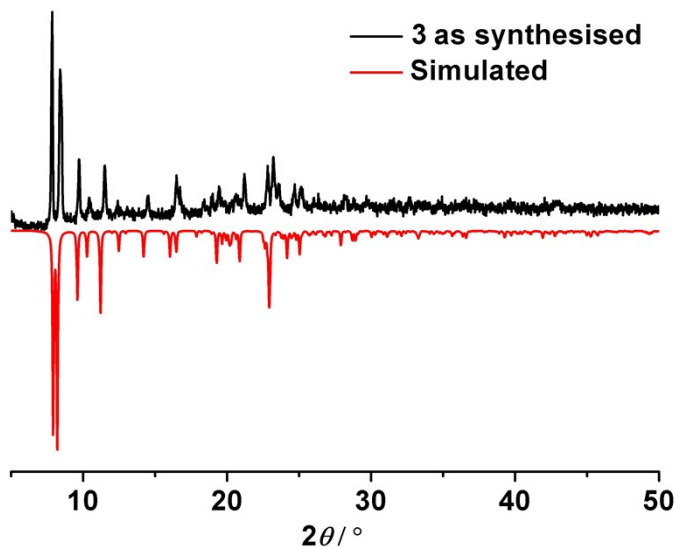


Fig. S3 PXRD patterns simulated from single crystal data and of polycrystalline samples of freshly synthesized of **1**, **2** and **3**.

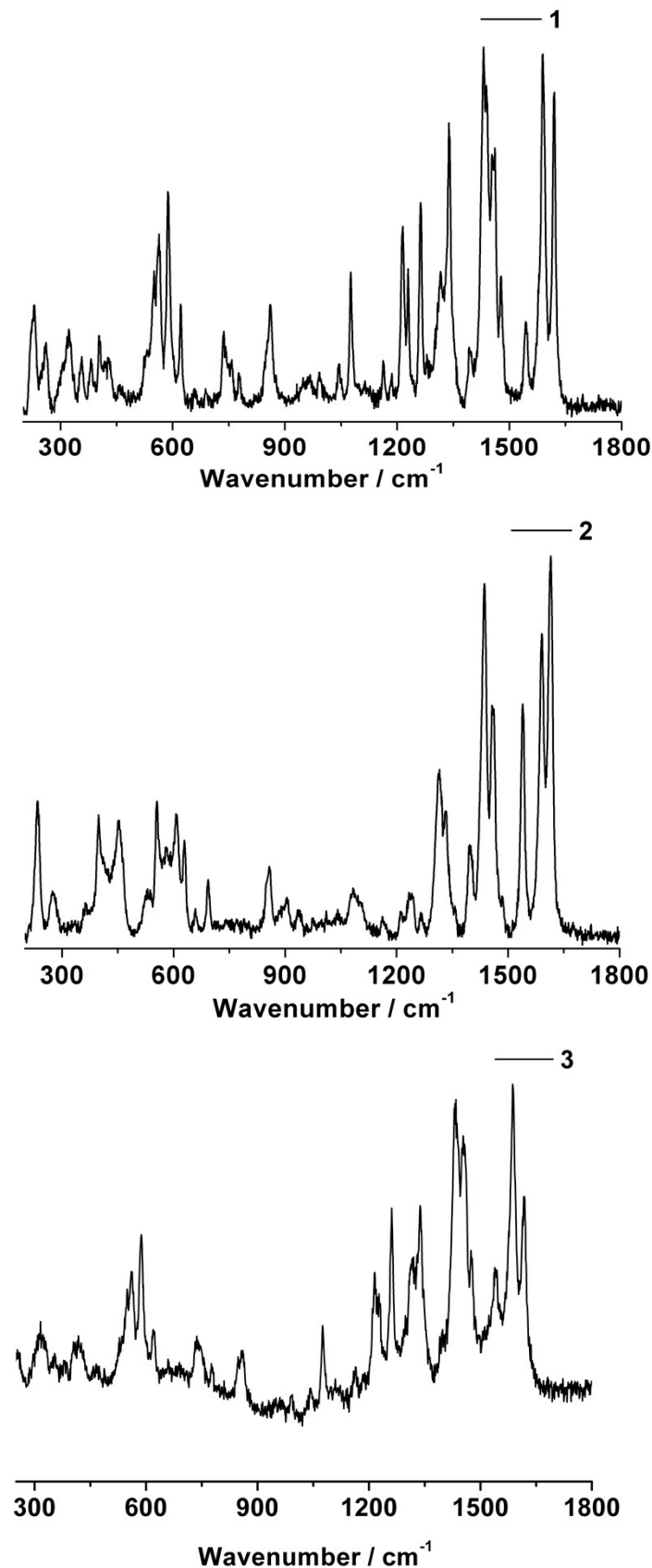


Fig. S4 Raman spectra of **1**, **2** and **3** ($\lambda = 514.5 \text{ nm}$).

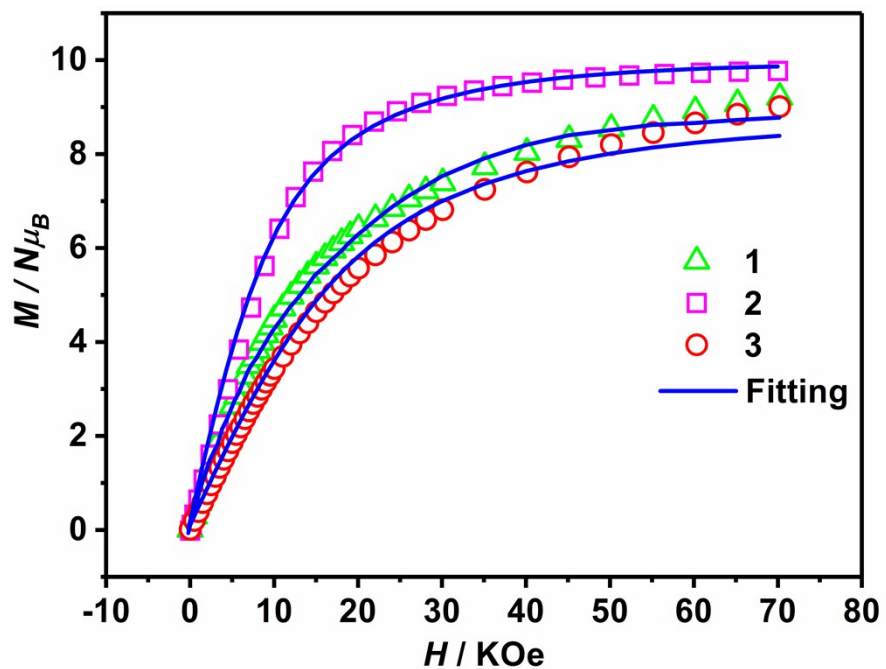


Fig. S5 Isothermal magnetizations for **1**, **2** and **3** at 1.8 K.

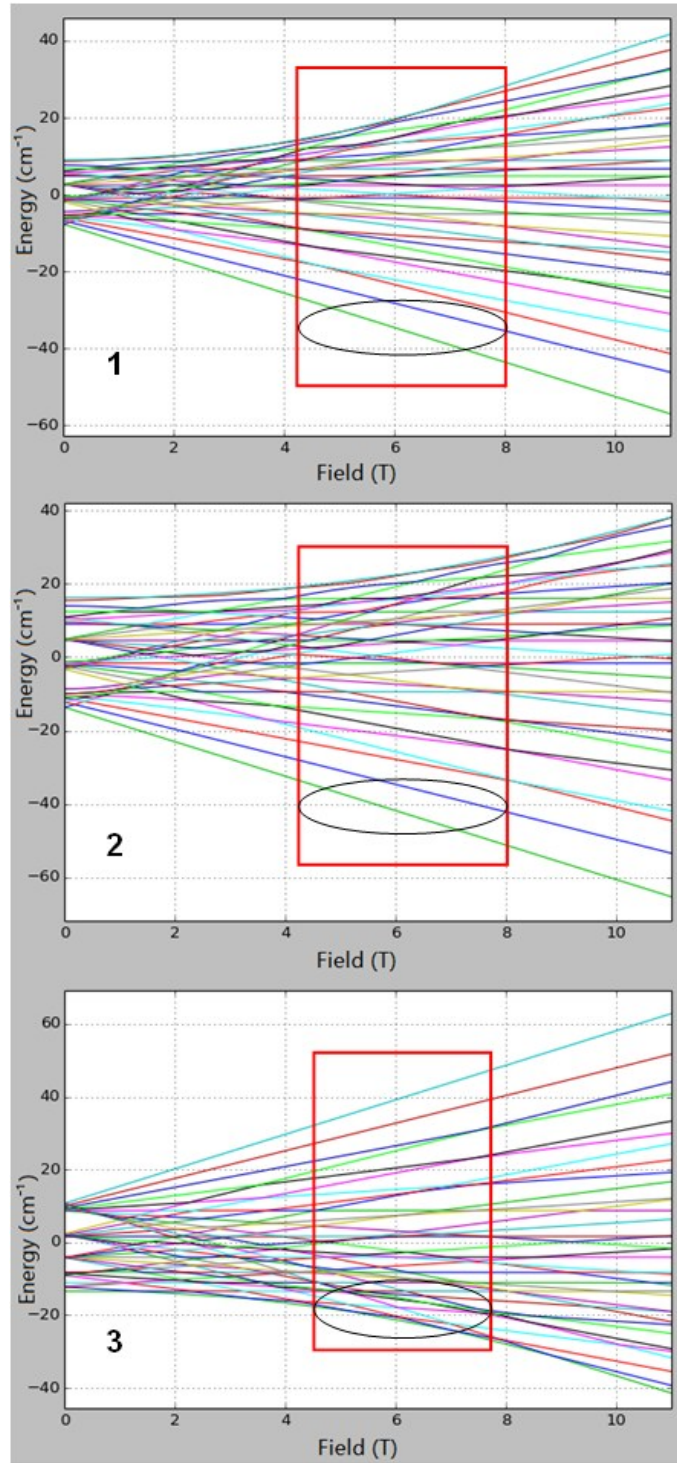


Fig. S6 Zeeman splitting of the Energy levels (in cm^{-1}) of **1**, **2**, and **3** with spin Hamiltonian parameters used in Fig. 4. Magnetic field is along the Fe-Fe directions. Red rectangle areas indicate the field ranges where the HF-EPR transitions can happen. Black circles point out the populated energy levels at 2 K. For **1** and **2**, the large dominate J values ($+0.47$ and $+0.86 \text{ cm}^{-1}$, respectively) result in the $S = 5$ as

pure ground states, hence the EPR spectrum at 2 K could be well described by $S = 5$, while for **3**, the dominate J (-0.72 cm^{-1}) results in severe crossing of low-lying energy states, and the EPR spectrum at 2 K is contributed by several low spin states ($S = 1, 2\dots$), making it difficult to simulate the spectra.

References

1. B. S. Snyder, G. S. Patterson, A. J. Abrahamson, R. H. Holm, *J. Am. Chem. Soc.*, 1989, **111**, 5214.
2. A. Elmali, Y. Elerman, I. Svoboda, H. Fuess, K. Griesar, W. Haase, *Z. Naturforsch B*, 1994, **49**, 365.
3. A. Elmali, Y. Elerman, I. Svoboda, H. Fuess, K. Griesar, W. Haase, *Z. Naturforsch B*, 1994, **49**, 1239.
4. S. Mukherjee, T. Weyhermüller, E. Bothe, P. Chaudhuri, *Eur. J. Inorg. Chem.* 2003, 1956.
5. Y. Yahsi, H. Kara, L. Sorace b, O. Buyukgungor, *Inorg. Chi. Acta* 2011, **366** 191.
6. N. Ademir, L. M. Rossi, I. Vencato, W. Haase, R. Werner, *J. Chem. Soc., Dalton Trans.*, 2000, 707.
7. S. Ménage, L. Que Jr, *Inorg. Chem.*, 1990, **29**, 4293.
8. G. J. Long, J. T. Wroblewski, R. V. Thundathil, D. M. Sparlin, E. O. Schlemper, *J. Am. Chem. Soc.*, 1980, **102**, 6040.
9. B. Chiari, O. Piovesana, T. Tarantelli, P. F. Zanazzi, *Inorg. Chem.*, 1982, **21**, 1396.
10. S. J. Barclay, P. E. Riley, K. N. Raymond, *Inorg. Chem.*, 1984, **23**, 2005.
11. A. Elmali, Y. Elerman, I. Svoboda, H. Fuess, K. Griesar, W. Haase, *Z. Naturforsch., Teil B*, 1994, **49**, 1239.
12. K.K. Nanda, S.K. Dutta, S. Baitalik, K. Venkatsubramanian, K. Nag, *J. Chem. Soc., Dalton Trans.* 1995, 1239.
13. J.A. Thich, C.C. Ou, D. Powers, B. Vasiliou, D. Mastropaoilo, J.A. Potenza, H.J.

- Schugar, *J. Am. Chem. Soc.*, 1976, **98**, 1425.
14. L.L. Borer, L. Thalken, C. Ceccarelli, M. Glick, J.H. Zhang, W.M. Reiff, *Inorg. Chem.*, 1983, **22**, 1719.
15. C.C. Ou, R.A. Lalancette, J.A. Potanza, H.J. Schugar, *J. Am. Chem. Soc.*, 1978, **100**, 2053.